Lung Nodule Detection of CT and Image-Based GLCM and RLM CT Scan Using the Support Vector Machine (SVM) Method

Za'imah Permatasari
Dept. of Electrical Engineering Institut Teknologi Sepuluh Nopember Surabaya, Indonesia
zaimah.permatasari@gmai.com

Mauridhi Hery Purnomo
Dept. of Electrical Engineering Institut Teknologi Sepuluh Nopember Surabaya, Indonesia
hery@ee.its.ac.id

I Ketut Eddy Purnama
Dept. of Electrical Engineering Institut Teknologi Sepuluh Nopember Surabaya, Indonesia
ketut@te.its.ac.id

***Abstract*- Lung cancer is a disease characterized by uncontrolled cell growth in lung tissue. If left untreated, this cell growth can spread out of the lungs through a process called metastasis to the nearest tissue or other part of the body.why lung cancer is one type of cancer that has a high mortality rate in the world. survey proved the most common cause of lung cancer is long-term exposure to tobacco smoke, which causes 80-90% of lung cancer. Non-smokers make up 10-15% of lung cancer cases, and these cases are usually caused by a combination of genetic factors, radon gas, asbestos, and air pollution, including passive cigarette smoke. That's why the number of deaths caused by lung cancer is so high. So to reduce the mortality rate, early detection needs to be done so that patients can be treated as quickly as possible. One of the detection processes carried out is by screening using Computed Tomography (CT) scan. Where (CT) itself uses a combination of X-ray or X-ray technology and a special computer system that allows to see the condition of the lungs from various angles and pieces, so that lung detection is more accurate. By using CT images, the level of malignancy of a nodule can be determined. This study aims to develop methods that can distinguish the characteristics of normal and non-pulmonary density densities. Cropping stage is done to get the Region of Interest (RoI) of pulmonary nodules. The segmentation stage is done to separate the area of the lesion from the background. The feature extraction stage is histogram based and Gray Level Co-occurrence Matrices. (GLCM) and RLM Texture feature values are then used as input to the classification stage of the method using Support Vector Machine (SVM).**

With detailed results (SVM) will produce accurate classification accuracy, then with accurate results that will make it easier for medical experts to identify the patient's lungs.

Keywords - Lung nodules, ROI, GLCM and RLM features, SVM

I. INTRODUCTION

The majority of lung cancer patients in Indonesia are active smokers. Heavy smokers have about a 10 times greater chance of developing lung cancer than nonsmokers. Lung cancer is classified into two groups, namely primary lung cancer and secondary lung cancer. Primary lung cancer is cancer cells originating from the lung, while secondary lung cancer is cancer cells that spread from other members of the body, including breast cancer and colon cancer (Sungging Haryo W., et al, 2011: 46). Primary lung cancer itself can be classified into two types, namely Non-small Cell Lung Cancer (NSCLC) and Small Cell Lung Cancer (SCLC). More than 80% of 2 cases of lung cancer are NSCLC types with subcategories of adenocarcinomas, squamous cell carcinomas, and large cell carcinomas. Early detection of lung cancer is very important to increase survival life. Early detection allows timely therapeutic intervention and improves prognosis in patients. Identifying this cancer at an early stage can increase a patient's 5-year life expectancy by up to 70%. The initial examination of patients clinically suspected of lung cancer is based on a chest radiograph. However, a chest X-ray has a low sensitivity to show significant lesions and has a high false-positive rate in detecting pulmonary nodules. States that 12-30% of lung cancer diagnoses are missed with a chest radiograph. One major diagnostic modality for lung cancer detection is a computerized tomography (Computerized Tomography). Keneko et al compared the superiority of chest CT scanning with chest X-ray on 1300 patients with a high risk of getting 15 lung cancer results detected on CT scan, which in 11 patients were not detected on chest radiograph (Icksan et al., 2008). One of the methods used to detect lung cancer is through a CT scan (Computed Tomography). Several studies have been developed to help classify lung cancer by several different methods, one of which is the classification of lung cancer cells using Artificial Neural Network (ANN) conducted by Zhou, et al (2002). Detection of lung cancer using fuzzy C-means and classification using Neural Networks was also carried out by Ramaraju, et al (2015). Another study was conducted by Devi Nurtiyasari (2014) using the Recurrent Neural Network and Recurrent Neuro-Fuzzy models for the classification of lung cancer nodules from lung images. In this study, the authors tried to detect pulmonary nodules.

Research carried out by Bhuvaneswari et al (Bhuvaneswari et al. 2014), classifies lung images automatically to recognize lung diseases namely Pleural Effusion, Emphysema, Bronchitis, and normal lungs. The initial stage is feature extraction using Gabor Filter and Walsh Hadamard transformation. The next stage is feature selection using Correlation-based Feature Selection (CFS) and Principal Component Analysis (PCA). The last stage is the classification process by comparing several methods such as Naïve Bayes, J48, K-NN, MLP. The results obtained show that PCA and MLP produce the highest accuracy which is 81%. While research conducted by Sergeeva et al (Sergeeva et al. 2016), classifies lung nodules by extracting features using texture and morphological features on CT scan images obtained

II. MATERIAL AND METHOD

2.1 *Material*

2.1.1 *Lungrounds*

Nodules Lung nodules areor ovals that are often found on X-ray or computed tomography (CT) scans. In one of the 500 Thoracic readings can be found a nodule. Maybe one or several nodules can be found when reading an X-ray from someone's piston.

2.1.2 *CTS can (Computed Tomography Scanner)*

CT scan (Computed Tomography Scanner) for the examination of all body organs, such as the arrangement of the central nerve, muscles, and bones, throat, abdominal cavity. This examination is intended to clarify the existence of a strong suspicion of an abnormality.

2.1.3 *Prepossessing*

To eliminate noise generated when Digital signals are obtained on the device, as well as to handle unwanted shapes on images consisting of two parts of Grayscale and Binary Image.

2.1.4 *Median Filter Median*

The filter is a method that focuses on the median value or the middle value of the total value of the entire pixel around it. Suppose there are data A = 1, B = 5, C = 2, D = 9, and E = 7, then the median filter will look for the middle value of all data that has been sorted in advance from the smallest to the largest data and then the middle value is taken (1,2,5,7,9). The median of the sequence is 5.

2.1.5 *Adaptive Histogram Equation An*

The image histogram is a graph that represents the relative frequency of occurrence of the pixel value of an image. Histogram modeling techniques can modify the image under the shape of the histogram, as desired.

2.1.6 *Connected Component Labeling Connected Component Labeling*

The algorithm is used to label each object in a binary image with a unique label. The grouping of pixels as an object is determined by their neighbor status.

2.1.7 *Features of the GLCM (Gray Level Cooccurrence Matrix)*

Features are unique characteristics of an object, features are divided into two, namely natural features and artificial features.

2.1.8 *RLM features (Run, Lenght, Matrix*)

Run-length matrix is a popular method for extracting textures to obtain statistical features or attributes contained in textures by estimating pixels that have the same degree of gray.

2.1.9 *Support Vector Machine (SVM)*

Support Vector Machine or SVM is one of the supervised learning models in machine learning.

2.1.10 *Receiver Operating Characteristics (ROC)*

Receiver Operating Characteristics (ROC) or also known as ROC graph or ROC curve, is a technique for measuring and visualizing the performance of a classification method. ROC can also be used to determine whether features used in a classification method can produce good classification results or not

2.2 Method

2.2.1 *Feature Extraction of Gray Level Co-occurrence Matrix (GLCM)*

Gray Level Co-occence Matrix (GLCM) is used to calculate gray-level spatial dependencies in an image. In GLCM the number of rows and columns is the same as the number of gray levels in the image. The joint event matrix is constructed in four spatial orientations (0º, 45º, 90º, and 135º). The next matrix is constructed as the average value of the previous matrix. The matrix is formed into variables Pi, j and the size of the matrix is NxN. Each element (i, j) represents the pixel frequency with gray levels i spatially related to pixels with gray levels j. The GLCM construction of a grayscale image is illustrated in Figure 3.1.

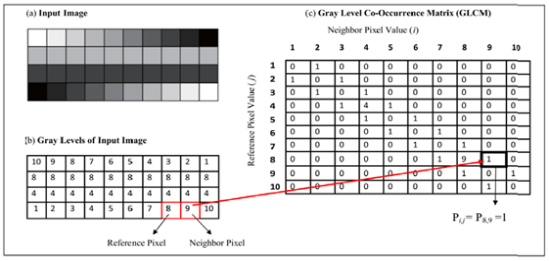

Figure 1. GLCM Construction

Equations used in the feature extraction process using GLCM, are as follows:

1. Contrast

$$\sum_{i,j=0}^{N-1} P_{i,j}\,(i-j)^2$$

(3.1)

2. *Correlation*

$$\sum_{i,j=0}^{N-1} P_{i,j}\left[\frac{(i-\mu_i)(j-\mu_j)}{\sqrt{(\sigma_i^2)(\sigma_j^2)}}\right]$$

(3.2)

3. *Dissimilarity*

$$\sum_{i,j=0}^{N-1} P_{i,j}\,|i-j|$$

(3.3)

4. *Energy*

$$\sum_{i,j=0}^{N-1} P_{i,j}^2$$

(3.4)

5. *Entrophy*

$$\sum_{i,j=0}^{N-1} P_{i,j}\,(-\ln P_{i,j})$$

(3.5)

6. *Homogeneity*

$$\sum_{i,j=0}^{N-1} \frac{P_{i,j}}{1+(i-j)^2}$$

(3.6)

7. *Mean*

$$\mu_i = \sum_{i,j=0}^{N-1} i\,(P_{i,j}) \quad , \quad \mu_j = \sum_{i,j=0}^{N-1} j\,(P_{i,j})$$

(3.7)

8. *Variance*

$$\sigma_i^2 = \sum_{i,j=0}^{N-1} P_{i,j}\,(i-\mu_i)^2 \quad , \quad \sigma_j^2 = \sum_{i,j=0}^{N-1} P_{i,j}\,(j-\mu_j)^2$$

(3.8)

9. *Standard Deviation*

$$\sigma_i = \sqrt{\sigma_i^2} \quad , \quad \sigma_j = \sqrt{\sigma_j^2}$$

(3.9)

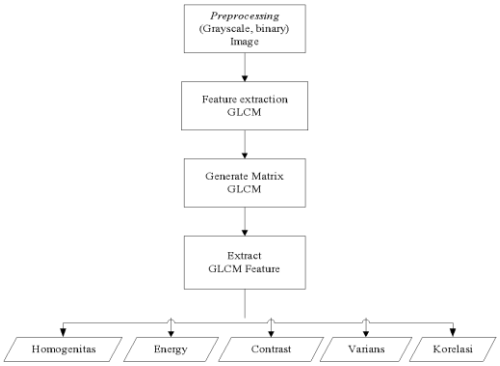

Figure 2. Steps in the GLCM feature extraction process

2.2.2 Run Feature Matrix Run Length Matrix (RLM)

P-value is used to indicate the RLM value, then Pij is an entry (i, j) to RLM. Additionally, use Nr to indicate length values *run* different that occur in ROI, and different sets of gray levels exist in ROI. And N becomes the total number of pixels in ROI.

$$N = \sum_{i \in N_g} \sum_{j \in N_r} j P_{i,j}$$

(3.10)

In calculating RLM in ROI, width, and height must be distinguished from the overall picture. ROI width is expressed in roi_width, the width of the entire width of the image measured in column figures. Likewise, roi_height is used for the height of the ROI and height of the image, which is measured by the row number. A pair in the form (dx, dy) is used to indicate direction. Following the convention in image processing that the pixel (0,0) is the upper-left corner, and the positive x-axis points to the right while the positive y-axis indicates weakness, it can be concluded that (dx, dy) = (1,0) means the horizontal direction (0 °) and (1, −1), (0, −1), (−1, −1) represent the anti-diagonal (45 °), vertical (90 °) and diagonal (135 °) directions, respectively. In this way, neighboring pixels in a given pixel (x, y) along the direction (dx, dy) can be calculated by the equation (x + dx, y + dy). Gray level values and pairs are *run-length* not always stored efficiently in memory

because they require two parallel arrays, the author uses one-to-one mapping to map pairs into integers expressed in the *pseudo-code* following.

Where roi_length is the *run* maximum length of ROI along the given direction. And can restore gray level or length *run*. RLM construction is carried out in two steps. Because ROI is carried out pixel by pixel to scan the entire image, resulting in overlap, as well as for gray level values and pairs *length run*. If an RLM is created for each ROI one by one by following each pixel in the ROI to calculate the length *run*, there will be many repetitive processes. Therefore, the author calculates the *length run* only once in the overall pixel in the image and stores the value in a separate array that has the same shape and size as the image.

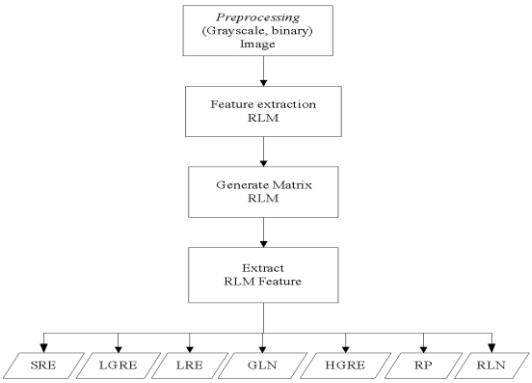

Figure 3. The steps in the RLM feature extraction process.

2.3.2 Classification of Cancer Images Using a Support Vector Machine (SVM)

The application concept of the SVM classifier is to determine the hyperplane based on its support vector ie the data closest to the other class. However, for the implementation of multi-class classification, it is necessary to have a kernel for modification, then it is known that the RBF (Radial Basis Function) kernel is the best for classification.

$$kernel\ RBFK\ =\ exp\ (-gg\ ||\ xxii-\ xxjj2), gg > 0 \quad (3.11)$$

(3.11)

In measuring the ability of the SVM algorithm to classify it is necessary to have an accuracy test of the results of the classification carried out with the algorithm. And see the potential of cancer in the test image between the image of the classification results with MRI data.

$$N\ =\ Z2\ (p)\ (q)\ /\ E^2 \quad (3.12)$$

This study uses an image dataset that has been prepared by the author consisting of normal and abnormal images. The dataset image is an MRI image of the lungs that identifies the lung that is affected by cancer and is normal. So class labeling is defined as normal and abnormal.

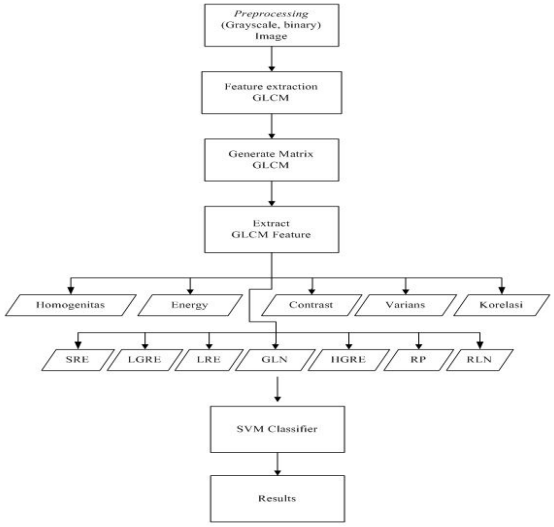

Figure 4. The steps in the SVM classification process

III. RESULT AND DISCUSSION

3.1 *Image Training Testing*

In the MRI medical image training process, the authors used two methods of GLCM and RLM to obtain information about the characteristics of the image. GLCM image features extraction process can be explained as follows:

1. Doing *resize* the image to a size of 100 x100
2. original image conversion options to the gray level using Matlab function rgb2gray.
3. Convert gray level to a binary image using Matlab im2bw function.
4. To filter the image using a median filter to dampen the *noise* contained in the image or in other words to get a finer image*(smooth)*using medfilt2 function.
5. Perform the feature extraction process by using the graycomatrix functionto obtain information about the characteristics of the image homogeneity, energy, contrast, correlation, mean i, mean j, variance.

RLM image features extraction process can be explained as follows:

1. Doing *resize* the image to a size of 100 x100

2. original image conversion options to the gray level using Matlab function rgb2gray.
3. Convert gray level to a binary image using Matlab im2bw function.
4. To filter the image using a median filter to dampen the *noise* contained in the image or in other words to get a finer image*(smooth)*using medfilt2 function.
5. Perform a feature extraction process to obtain information about the characteristics of SRE1, LRE1, GLN1, RP1, RLN1, LGRE1, HGRE1 images.

Tests on the image feature extraction process can be explained step by step in the test drawings Figure 4.1 - 4.3. In Figure 4.1 explains the original CT Scan image that will be *processed*.

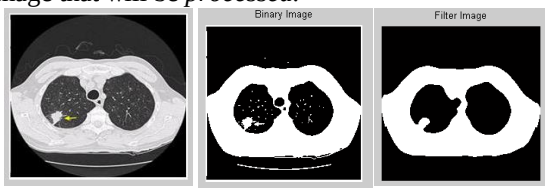

Figure 4.3 Filter Image The

The results of GLCM feature extraction based on the image that has been *processed* to obtain homogeneity, energy, contrast, variance, and correlation values obtained results shown in Figure 4.4.

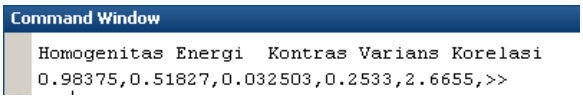

Figure 4.4 The result of feature extraction GLCM

RLM feature extraction results by the image that has been done *processing* to get the value SRE1, LRE1, GLN1, RP1, RLN1, LGRE1, and HGRE1 obtained the results shown in Figure 4.5.

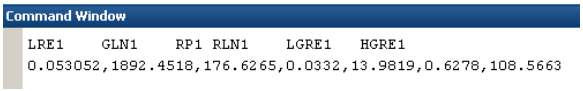

Figure 4.5 RLM feature extraction

results The results of the feature extraction process for all data prepared by the data author are seen in the following test image.

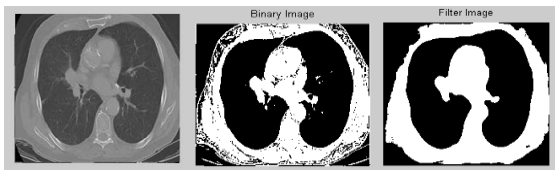

Figure 4.6 Original normal binary, image and filter results

imageFrom the results of the extraction of the overall image features can be presented in the feature extraction table Table 4.1.

H	E	C	Var	Cor	sre1	Lre 1	gnl1	rp1	rln1	lgre1	hgre1
1.0	0.5	0.0	0.3	2.6	0.1	496.4	290.7	0.1	18.1	0.6	125.6
1.0	0.5	0.0	0.3	2.5	0.1	1350.5	193.9	0.0	15.2	0.6	125.7
1.0	0.5	0.0	0.3	2.7	0.0	853.0	252.3	0.0	18.3	0.6	115.2
1.0	0.5	0.0	0.2	2.7	0.0	568.4	279.3	0.1	29.0	0.6	118.3
1.0	0.6	0.0	0.2	2.8	0.0	1101.7	222.8	0.0	12.8	0.6	110.9
1.0	0.6	0.0	0.2	2.8	0.0	1371.0	203.2	0.0	19.2	0.6	107.1
1.0	0.5	0.0	0.3	2.5	0.0	715.7	237.2	0.0	16.3	0.5	140.7
1.0	0.5	0.0	0.2	2.7	0.0	1232.9	221.9	0.0	15.4	0.6	110.7
1.0	0.6	0.0	0.2	2.8	0.0	1211.8	218.1	0.0	15.9	0.6	110.0
1.0	0.6	0.0	0.2	2.8	0.1	1042.0	229.8	0.0	16.0	0.6	120.8
1.0	0.5	0.0	0.3	2.7	0.1	1892.5	176.6	0.0	14.0	0.6	108.6
1.0	0.5	0.0	0.3	2.6	0.0	737.1	250.4	0.0	19.0	0.6	125.7
1.0	0.5	0.0	0.2	2.7	0.1	2074.5	174.7	0.0	16.2	0.7	99.7
1.0	0.5	0.0	0.3	2.6	0.1	1037.2	225.9	0.0	15.2	0.6	123.5

3.2 Image Classification Testing

In the testing process of CT Scan medical image classification, the extraction method the image feature uses two methods of GLCM and RLM to get information about image characteristics. The first step is to resize the image to a size of 100x100 followed by the process of the grayscale image to get the image in gray degrees. The grayscale image is carried out by conversion to binary process to get a firm variable in black or white values in B / W color format. In the BW image of the process, a filter is needed to suppress the noise level to obtain a cleaner image to facilitate the classification process. Noise filter used is a 2d median filter. Figure 4.20 shows a GUI for testing CT Scan image classification.

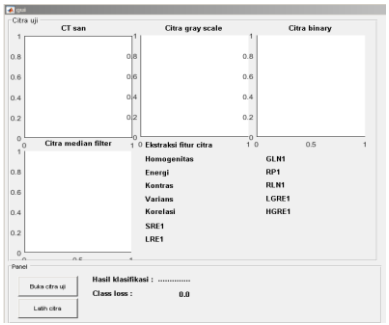

Figure 4.20 SVM Image Classification GUI

In the first test, the writer chooses the test image which is done by pressing the open image test button, so the image results will appear *processing* in the GUI shown in Figure 4.21.

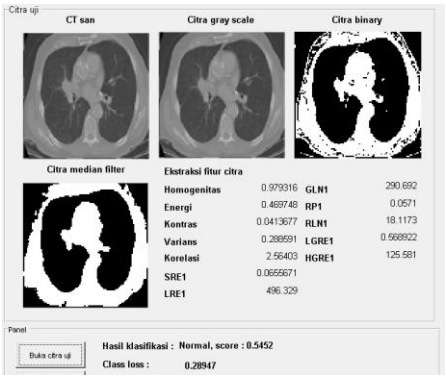

Figure 4.21results processing Test image1

In the GUI the results of *processing* and extraction results of test 1 image features are shown by the parameters of homogeneity, energy, contrast, variance, correlation, SRE1, LRE1, GLN1, RP1, RLPN1, LGRE1, and HGRE1. The results of the image classification test process are shown in Figure 4.22, where image 1 is class 1 which is defined as a non-cancer class.

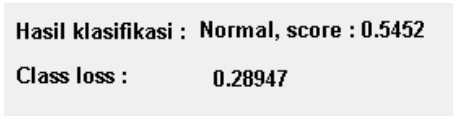

Figure 4.22 Test image classification results in 1

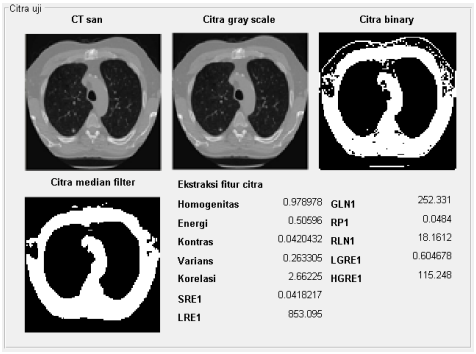

Figure 4.25 results *processing* Test image3 The

GUI shows the results of the *processing* and extraction results of test 3 image features indicated by the values of the parameters of homogeneity, energy, contrast, variance, correlation, SRE1, LRE1, GLN1, RP1, RLPN1, LGRE1, and HGRE1. The results of the image classification test process are shown in Figure 4.26, where image 3 is class 1 which is defined as a non-cancer class.

Figure 4.26 Test image classification results in 3

Figure 4.30 Test image classification results in 5

In the sixth test, the authors chose the test image which is done by pressing the open image test button, so the image results will appear *processing* in the GUI shown in Figure 4.31.

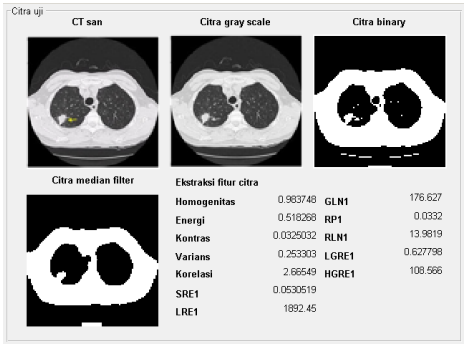

Figure 4.31results *processing* Test image6

The GUI shows the results *processing* and the extraction results of test image 6 features indicated by the value of the parameters of homogeneity, energy, contrast, variance, correlation, SRE1, LRE1, GLN1, RP1, RLPN1, LGRE1, and HGRE1. The results of the image classification test process are shown in Figure 4.32, where image 6 is class 2 which is defined as a cancer class.

Figure 4.32 Test image classification results from 6

In the seventh test, the authors chose the test image which is done by pressing the open image test button,

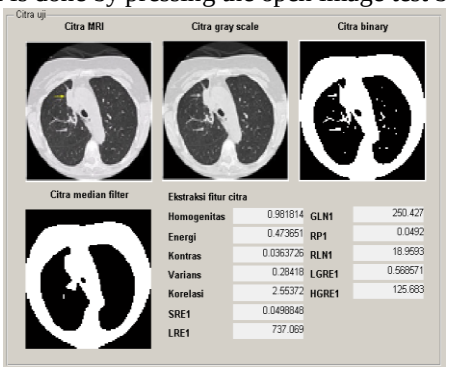

Figure 4.33results *processing* Test image7

In the GUI, the results of *processing* and extraction results of test 7 image features are shown by the parameters of homogeneity, energy, contrast, variance, correlation, SRE1, LRE1, GLN1, RP1, RLPN1, LGRE1, and HGRE1. The results of the image classification test process are shown in Figure 4.34, where image 7 is class 2 which is defined as a cancer class.

Figure 4.34 Test image classification results in 7

Figure 4.40results *processing* Test image10

In the GUI the results of *processing* and extraction results of the test image 10 features are shown by the parameters of homogeneity, energy, contrast, variance, correlation, SRE1, LRE1, GLN1, RP1, RLPN1, LGRE1, and HGRE1. The results of the image classification test process are shown in Figure 4.41, where image 10 is class 2 which is defined as a cancer class.

Figure 4.40 Test image classification results in 10

Based on ten test results can be made a table to show the level of success of the CT scan image classification that has been done.

Table 4.1 Table of test results imagery MRI

No	test image	Score	Loss class	image	Prediction	Result
1	Image 1	0.5452	0.2895	1	1	Normal
2	Image 2	0.1985	0.2895	1	1	Normal
3	image 0.7454 0.3158		3	1	1	Normal
4	image 0.2895	0.47	4	1	1	Normal
5	image 0.5843 0.2895		5	1	1	Normal

Image training results using SVM will produce support vectors for positive and negative because it can give a picture of two hyperplanes that pass through at least one positive instance and one negative instance each for each of them hyperplanes separated by distances. SVM will maximize the distance between the two hyperplanes while maintaining each class instance on both sides of the two hyperplanes as much as possible. Table 4.2 is the verctor support value for both negative and positive classes. **Tabel 4. 3** Tabel hasil pengujian citra CT SCAN

No	Negatif kelas	Positif kelas
1	0.557	0.443
2	0.4258	0.5742
3	0.2571	0.7429
4	0.603	0.397
5	0.6146	0.3854
6	0.4499	0.5501
7	0.6086	0.3914
8	0.4618	0.5382
9	0.5899	0.4101
10	0.5903	0.4097
11	0.1841	0.8159
12	0.2055	0.7945
13	0.2055	0.7945
14	0.1935	0.8065
15	0.2056	0.7944
16	0.2055	0.7945
17	0.2055	0.7945

From the table of positive and negative class can be made a scatter graph that illustrates the spread of the values of the two classes.

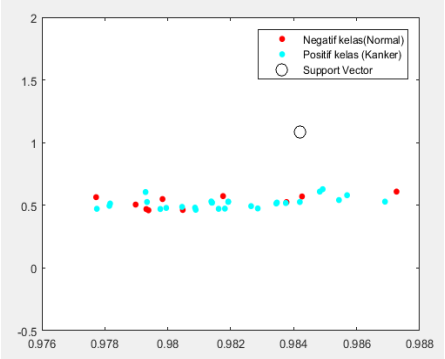

Figure 4. 41 SVM scatter graph of negative and positive classes

IV. Conclusion and suggestion

The conclusions obtained can be mentioned, namely:

1. Because the texture feature extraction method tends to get the texture characteristics of the CT Scan image However, using a combination of extraction features of GLCM and RLM can improve classification accuracy. This is explained by increasing the number of features that can be extracted by using two methods of feature extraction.

2. The appearance of noise in an MRI image can be denoised using a median filter with thresholding set to obtain a cancer object which is said to be an optimal metric value [4 4]. Three holding values that are too high result in the loss of cancer objects from the MRI image, failing the classification process.

3. The image feature extraction results are used to train SVM classifiers with RBF kernel which successfully classifies CT Scan images of lung cancer as normal or cancerous.

4. The accuracy of SVM classification results obtained 100%, the results of an accurate SVM classification can be used by medical experts to help identify abnormalities that may exist in the lungs of patients. Identification of errors in conventional MRI images, it is very difficult to obtain accurate analysis results because in CT scan images there are many image slices with complex patterns.

REFERENCES

[1] World Health Organization, "Cancer facts sheet, 2012."[Online].Available:http://www.who.int/mediacentre/factsheets/fs297/en/. [Accessed:25-May-2015].
[2] M. J. Cochrane and S. I. Lee, "Evaluating Pulmonary Nodules," A Newletter for Referring Physicians, vol. 4, no. 8, Aug-2006.
[3] L. Fan, S. Y. Liu, Q. C. Li, H. Yu, and X. S. Xiao, "Multidetector CT features of pulmonary focal ground-glass opacity: Differences between benign and malignant," Br. J. Radiol., vol. 85, no. July, pp. 897–904, 2012.
[4] T. Eguchi, A. Yoshizawa, S. Kawakami, H. Kumeda, T. Umesaki, H. Agatsuma, T. Sakaizawa, Y. Tominaga, M. Toishi, M. Hashizume, T.Shiina, K. Yoshida, S. Asaka, M. Matsushita, and T. Koizumi, "Tumor Size and Computed Tomography Attenuation of Pulmonary Pure Ground-GlassNodules Are Useful for Predicting Pathological Invasiveness," PLoS One, vol. 9, no. 5, p. e97867, 2014.
[5] F. Li, S. Sone, H. Abe, H. Macmahon, and K. Doi, "Malignant versus benign nodules at CT screening for lung cancer: comparison of thin-sectionCT findings.," Radiology, vol. 233, no. 1, pp. 793–798, 2004.
[6] S. Sivakumar, C. Chandrasekar, and A. L. Cancer, "Lung Nodule Detection Using Fuzzy Clustering and Support Vector Machines," Int. J. EnginneeringTechnol., vol. 5, no. 1, pp. 179–185, 2013.
[7] R. S. Kennedy, N. E. Lane, K. S. Berbaum, and M. G. Lilienthal.1993. Simulator Sickness Questionnaire: An Enhanced Method for QuantifyingSimulator Sickness. The International Journal of AviationPsychology, vol. 3, pp. 203–220
[8] Golding,J.F.1998. Motion sickness susceptibility questionnaire revised and its relationship to other forms of sickness. Brain Research Bulletin
47(5):507-516
[9] Toet,Alexander.2008. Cybersickness and Desktop Simulations: Field ofViewEffects andUser Experience. Proc. SPIE Vol. 6957-21, EnhancedandSynthetic Vision 2008, Orlando FL, USA, March 2008
[10] Dennison,Mark.S.2015. Use of physiological signals to predictcybersickness. University of California, Irvine 92627 Irvine, CA, USA
[11] Kim et al.2015. Characteristic changes in the physiological componentsof cybersickness. Psychophysiology, 42 (2005), 616–625. BlackwellPublishin Inc. Printed in the USA.
[12] Niedermeyer E.; da Silva F.L.2004. Electroencephalography:
BasicPrinciples, Clinical Applications, and Related Fields. LippincottWilliams & Wilkins. ISBN 0-7817-5126-8.
[13] Klem, G.H., Luders, H.O., Jasper, H.H., Elger, C., 1999. The ten–twentyelectrode system of the International Federation. The InternationalFederation of Clinical Neurophysiology. Electroencephalogr.Clin.Neurophysiol., Suppl. 52, 3–6.
[14] Trans Cranial Technologies, 10/20 System Positioning Manual, Whancai : Hongkong
[15] Jonke, Robert.2014. Feature Extraction and Selection for EmotionRecognition from EEG. IEEE TRANSACTIONS ON AFFECTIVECOMPUTING, VOL. 5, NO. 3, JULY-SEPTEMBER 2014